

FAIR: Facilitating Artificial Intelligence Resilience in Manufacturing Industrial Internet

Yingyan Zeng¹, Ismini Lourentzou², Xinwei Deng³, and Ran Jin³

¹University of Cincinnati

²University of Illinois

³Virginia Tech

March 4, 2025

Abstract

Artificial intelligence (AI) systems have been increasingly adopted in the Manufacturing Industrial Internet (MII). Investigating and enabling the AI resilience is very important to alleviate profound impact of AI system failures in manufacturing and Industrial Internet of Things (IIoT) operations, leading to critical decision making. However, there is a wide knowledge gap in defining the resilience of AI systems and analyzing potential root causes and corresponding mitigation strategies. In this work, we propose a novel framework for investigating the resilience of AI performance over time under hazard factors in data quality, AI pipelines, and the cyber-physical layer. The proposed method can facilitate effective diagnosis and mitigation strategies to recover AI performance based on a multimodal multi-head self latent attention model. The merits of the proposed method are elaborated using an MII testbed of connected Aerosol[®] Jet Printing (AJP) machines, fog nodes, and Cloud with inference tasks via AI pipelines.

Keywords: Manufacturing Industrial Internet, Multi-head Self Latent Attention, Resilience of Artificial Intelligence

1 Introduction

A Manufacturing Industrial Internet (MII) connects manufacturing equipment, physical processes, systems, and networks via ubiquitous sensors, actuators, and computing units [Chen et al., 2018]. By enabling the seamless collection of high-speed, large-volume data, MII establishes the digital foundation necessary for deploying Artificial Intelligence (AI) models that deliver critical computational services, such as quality modeling, process variation analysis, fault prognosis and diagnosis, and optimization [Arinez et al., 2020], which enhance manufacturing efficiency, reduce operational costs, and enable intelligent automation.

As AI becomes increasingly integrated into manufacturing decision-making within MII, ensuring the resilience of AI systems is critical for maintaining reliable and continuous computation services [Chen and Jin, 2020]. In the context of MII, an AI system consists of three interconnected layers: (i) the data layer, representing the collected manufacturing data; (ii) the AI pipeline layer, where data are processed via the deployed AI models and pipeline ranking systems [Chen and Jin, 2020]; (iii) the cyber-physical layer, encompassing the Fog-Cloud computing infrastructure that supports the communication and computation in the system [Wang et al., 2020, Chen and Jin,

2024]. Thereafter, AI systems face challenges from three primary types of root causes, each tied to a critical system component: (i) data quality issues; (ii) AI model singularity; and (iii) cyber-physical layer failures. These hazards can lead to severe AI modeling performance degradation, resulting in incorrect predictions, faulty decisions, and economic losses. Therefore, it is necessary to develop a comprehensive framework that formally defines AI resilience in MII, quantifies the resilience performance, and proposes mechanisms for detecting and mitigating hazards in AI systems.

In the literature, system resilience is generally defined as a system’s ability to withstand, respond to, and recover from unexpected disruptions (*i.e.*, hazards) [Poulin and Kane, 2021]. To evaluate the resilience of general infrastructure systems designed to provide continuous services [Hall et al., 2016], resilience curves have been widely studied to derive magnitude-based, duration-based, rate-based, and threshold-based metrics [Poulin and Kane, 2021, Cheng et al., 2023]. In the context of MII, a closely related domain is Internet-of-Things (IoT) systems, where resilience is linked with attributes such as confidentiality, integrity, reliability, maintainability, and safety [Berger et al., 2021]. While existing frameworks provide a foundation for understanding AI system resilience in MII, they lack an approach that addresses the unique challenges of AI systems under the influence of three key interconnected layers. Despite the importance of resilience, most AI evaluation frameworks remain narrowly anchored to static performance metrics (*e.g.*, accuracy, precision) [Flach, 2019]. These metrics, while useful for offline model validation, provide limited insight into how AI systems degrade, adapt, or recover when confronted with heterogeneous disruptions in an online computation service in MII. Compounding this issue is the absence of quantitative resilience metrics for AI systems in MII. Furthermore, limited studies substantiate these frameworks with empirical demonstrations and experimental validation, hindering further diagnosis and mitigation efforts.

The objective of this work is to create a novel framework of resilient AI in MII which aims to (i) create quantitative metrics to evaluate the resilience of the AI system; (ii) diagnose root causes of AI system performance degradation; and (iii) automate context-aware mitigation strategies for the failures. The proposed framework will establish a solid foundation for understanding, quantifying, and improving the resilience of the AI systems in MII.

To achieve the objective, we first identify and categorize the different types of root causes that affect each of the three layers of an AI system in MII. Building on the taxonomy of failures and informed by the literature on infrastructure resilience, we consider two new metrics: temporal resilience and performance resilience to jointly quantify the AI system’s capacity to absorb and recover from hazards arising from the identified root causes. Moreover, the proposed framework focuses on detecting failures and identifying their root causes to enable timely mitigation strategies that enhance system stability. It is known that the MII’s integrated digital infrastructure can enable a seamless collection of runtime metrics of computation nodes, including CPU and memory utilization, download and upload bandwidths, along with performance from AI pipeline. Such information provides granular visibility of the system, which serves as a “side channel” to detect and diagnose hazards. However, the high-dimensional multimodal runtime data pose significant challenges for constructing proper diagnosis models, where multiple root causes can occur simultaneously. To address these challenges, we propose a Multimodal Multi-head Self Latent Attention (MMSLA) model to accurately diagnose root causes by capturing the dependencies between latent features associated with different root causes. Finally, mitigation strategies for different failure scenarios are developed based on several promising approaches from literature. The effectiveness of the resilience metrics, MMSLA model, and mitigation actions is evaluated within an MII environment comprising Cloud computing and fog nodes.

The remainder of this paper is organized as follows. Section 2 introduces the proposed resilient AI

framework. Section 3 evaluates the performance of the framework with a comprehensive MII case study for Aerosol Jet® Printing (AJP) process quality modeling. We conclude the work with some discussion of future work in Section 4.

2 Methodology

2.1 The AI System and Resilience Metrics In MII

The AI system in MII consists of three layers: data layer, AI pipeline layer, and cyber-physical layer. In this study, we focus on the AI system that provides supervised learning-based computation services (*e.g.*, quality modeling). As shown in Fig. 1, sensor data collected via MII during manufacturing processes are stored in the local database. The collected data serves as input to the AI pipeline, which processes it through a sequence of steps to support online decision-making. Specifically, we focus on multivariate time series classification pipelines, which consist of data augmentation, standardization, and Deep Neural Network (DNN) classifiers [Shojaee et al., 2021]. The AI pipelines are ranked and trained in the Cloud using historical data and then deployed in the cyber-physical network for real-time inference. The Cloud functions both as an orchestrator, assigning computation tasks to nodes, and as a computation node, executing tasks as needed. The fog nodes (*e.g.*, digital signal processors and GPUs) are positioned close to the machines for efficient processing with low communication latency. They execute the deployed AI pipelines and return results to the Cloud for further analysis and decision-making.

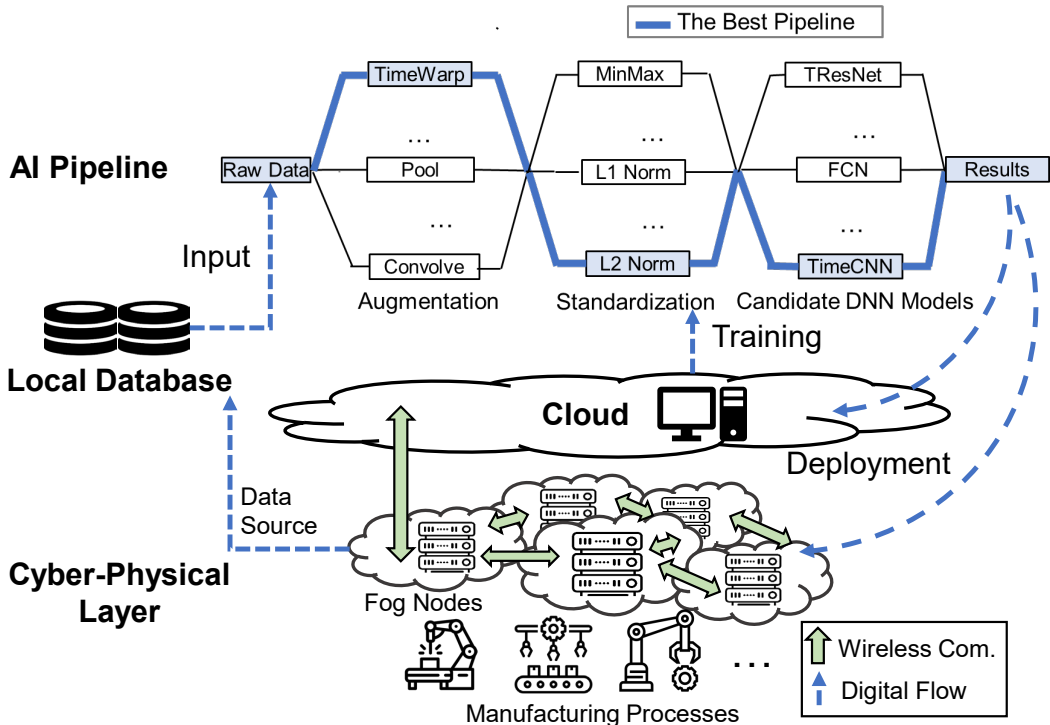


Figure 1: The AI system in Manufacturing Industrial Internet

The AI system’s performance is measured by metrics, including accuracy, precision, F1 score of each supervised learning task over the operation time, which should remain within an expected range under normal conditions. To quantify the system’s resilience under hazards, we identify

Table 1: The proposed resilience metrics.

Category	Metrics	Expression	Definition
Temporal Resilience	Failure Duration (FD)	$t_3 - t_1 \downarrow$	Duration of Hazard Period and Recovery Period
	Recovery Efficiency (RE)	$(t_3 - t_2)/(t_3 - t_1) \uparrow$	Ratio of Recovery Time to Total Failure Duration
	Performance Retention (PR)	$\int_{t_1}^{t_3} P_t / (t_3 - t_1) \uparrow$	Average Performance during Failure
Performance Resilience	Restoration Rate (RR)	$\int_{t_3}^{t_3+\Delta t} P_t / \int_{t_1}^{t_1-\Delta t} P_t \uparrow$	Restored Performance Relative to Pre-failure Baseline

key root causes from each layer that may impact performance. In the data layer, performance degradation can arise from (i) sensor contamination or failure, resulting in inaccurate measurements or missing data in several modalities [Liu et al., 2020]; (ii) sensor degradation and calibration issues may cause a low signal-to-noise ratio (SNR), which makes it difficult for AI systems to distinguish meaningful variations from noise [Montgomery, 2009]; (iii) data distribution shifts in input variables occur due to manufacturing customization, where process settings are adjusted to accommodate different product specifications, potentially leading to time varying data distributions [Li et al., 2022]; (iv) imbalanced class distribution in the data, where data from conforming processes significantly outweighs nonconforming samples [Liu et al., 2022, Zeng et al., 2023a,b]. Within the AI pipeline layer, a critical hazard arises from structural instability in model architectures, which we refer to as model singularity. The model’s parameters or mathematical structure become degenerate, resulting in issues such as vanishing/exploding gradients during optimization [Tan and Lim, 2019], which manifest as erratic predictions (*e.g.*, NaN values or extreme outliers) during inference [Hanin, 2018]. In the cyber-physical layer, we consider two primary hazards: (i) communication channel disruptions, triggered by cyber-attacks such as distributed denial-of-service (DDoS) intrusions [Lo et al., 2010], and (ii) fog node failures, caused by hardware degradation and failure (*e.g.*, overheating, memory leaks) or software-induced resource exhaustion. These hazards degrade real-time inference capabilities, manifesting as latency spikes, data packet loss, or unplanned downtime. In summary, hazards across the three layers degrade AI system performance in MII, manifesting in distinct ways: data-layer disruptions corrupt input integrity, pipeline-layer instabilities induce erratic predictions, and cyber-physical failures cripple real-time inference.

To evaluate the resilience of the AI systems against such hazards, we propose two metrics: temporal resilience and performance resilience to quantify the impact and how the AI system recovers from the failures. Inspired by [Cheng et al., 2023], Fig. 2 shows an example of the performance curve of an AI system during its operation. Let P_t denote the performance of the AI system at time t (*e.g.*, classification accuracy for quality modeling), and P_S represent the minimum satisfactory threshold in the computation service. Under normal operation, $P_t \geq P_S$. When a hazard factor is applied to the AI system, the hazard-triggered failure occurs at t_1 when $P_t < P_S$. After detecting the failure and diagnosing the root cause, mitigation begins at t_2 , which restores the system’s performance to the desired level P_S by t_3 .

As detailed in Table. 1, temporal resilience quantifies recovery speed through two dimensions: the failure duration as the total downtime from hazard onset to full recovery (shorter is better), and recovery efficiency, which reflects how effectively the system restores operation (higher is better). Performance resilience, on the other hand, assesses decision-making robustness of the system via the

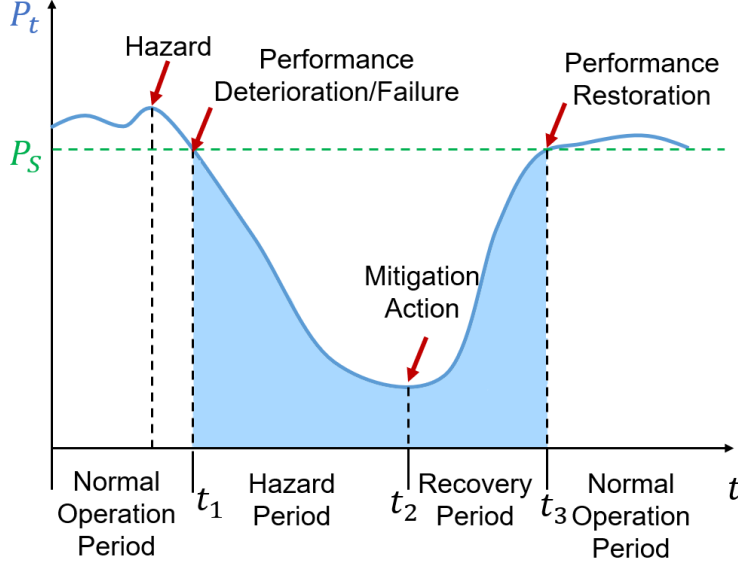


Figure 2: AI system subject to performance deterioration and recovery actions in MII.

performance retention and performance restoration rate (both higher is better). Together, these metrics assess how AI systems withstand, adapt to, and recover from hazards comprehensively.

2.2 A Multimodal Multi-head Self Latent Attention Model for Root Cause Diagnosis

Achieving high resilience in AI systems hinges on precise root-cause diagnosis across data, model, and cyber-physical layers, ensuring correct mitigation actions align with the underlying failure mode. To provide accurate diagnosis across multiple root causes based on multimodal data with varying and high dimensions, we propose the MMSLA model (Fig. 3) to predict the root cause types based on runtime metrics and performance of the computation task as input. The MMSLA encodes the input data from multiple modalities into a lower-dimensional latent space and employs a set function-based neural network to standardize varying dimensions across samples. Multi-head attention is then applied to the latent variables, with each head focusing on a specific factor, enabling the model to simultaneously learn distinct correlations between latent variables for each root cause.

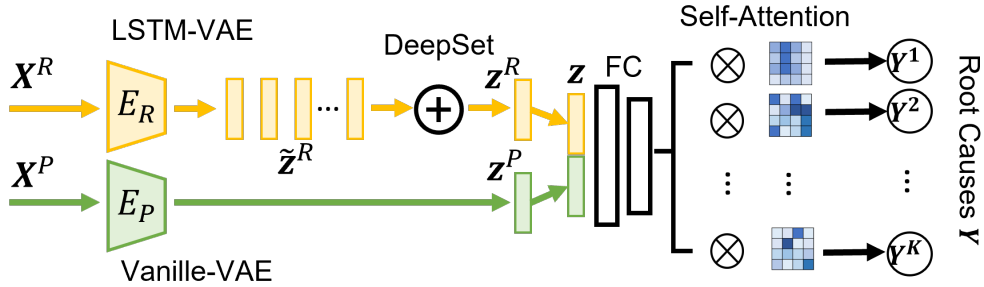


Figure 3: The proposed MMSLA model

In the AI system in MII, we assume the computation service is provided for a batch of data each

time. After completing a computation task i , the supervised learning performance $\mathbf{X}_i^P \in \mathbb{R}^P$ is sent to the Cloud, where P represents the performance metrics’ dimension. Meanwhile, the assigned computation node collects runtime metrics as $\mathbf{X}_i^R \in \mathbb{R}^{n_i \times R}$, where n_i is the number of timestamps for task i , and R is the number of monitored runtime metrics.

To fuse the information from both modalities, the MMSLA model first encodes \mathbf{X}_i^P and \mathbf{X}_i^R by an LSTM-Variational Autoencoder (VAE) $E_R(\cdot)$ [Wang et al., 2017] and a vanilla VAE $E_P(\cdot)$ [Kingma, 2013], respectively. Let n be the sample size, *i.e.*, the number of executed computation tasks. $E_P(\cdot)$ encodes \mathbf{X}^P to a latent variable $\mathbf{z}^P \in \mathbb{R}^{n \times u^P}$, where u^P is the latent dimension. Similarly, $E_R(\cdot)$ encodes \mathbf{X}^R to $\tilde{\mathbf{z}}^R \in \mathbb{R}^{n \times n_i \times u^R}$ with u^R as the latent dimension. During the process, the VAE loss is employed on each modality, which minimizes the Kullback-Leibler (KL) divergence:

$$\begin{aligned} \mathcal{L}^{VAE} = & -\mathbb{E}_{q_\phi(\mathbf{z}^P|\mathbf{x}^P)} [\log p_\theta(\mathbf{X}^P | \mathbf{z}^P)] \\ & - \mathbb{E}_{q_\phi(\tilde{\mathbf{z}}^R|\mathbf{x}^R)} [\log p_\theta(\mathbf{X}^R | \tilde{\mathbf{z}}^R)] \\ & + \alpha D_{KL}(q_\phi(\mathbf{z}^P | \mathbf{X}^P) \| p_\theta(\mathbf{z}^P)) \\ & + \alpha D_{KL}(q_\phi(\tilde{\mathbf{z}}^R | \mathbf{X}^R) \| p_\theta(\tilde{\mathbf{z}}^R)), \end{aligned} \quad (1)$$

where $q_\phi(\mathbf{z}|\mathbf{x})$ approximates the true latent distribution $p_\theta(\mathbf{z})$, and $\alpha \geq 0$ is the weight for KL loss. Here the same weight is used for each modality to encourage a balanced latent representation.

To standardize the varying dimension n_i , a canonical model architecture, DeepSet [Zaheer et al., 2017], is applied to $\tilde{\mathbf{z}}^R$, mapping it to $\mathbf{z}^R \in \mathbb{R}^{n \times u^R}$. In particular, the DeepSet model is a set function $f(S) = \rho(\sum_{\tilde{\mathbf{z}}^R \in S} \phi(\tilde{\mathbf{z}}^R))$, where both ρ and ϕ are neural networks. Hereby, the latent vectors \mathbf{z}^P and \mathbf{z}^R are concatenated as latent features \mathbf{Z} . To capture root cause-specific feature importance and inter-latent variable dependencies, we propose to use a multi-head self attention mechanism, where each head focuses on the dependencies associated with a specific root cause. This approach jointly models latent variables across all root causes, providing greater efficiency than developing separate diagnosis models for each root cause. Additionally, by learning from shared latent representations, the model effectively captures correlations between root causes, enhancing diagnostic accuracy.

Let K be the number of all root causes of different types. For root cause j , the following layer is applied to the latent features:

$$f_{\text{att}}^j(\mathbf{Z}) = \mathbf{Z} \odot \text{softmax}\left(\mathbf{W}_{f_{\text{att}}}^j \mathbf{Z} + \mathbf{b}_{f_{\text{att}}}^j\right), \quad (2)$$

where the weight matrix $\mathbf{W}_{f_{\text{att}}}^j \in \mathbb{R}^{(u^P+u^R) \times (u^P+u^R)}$, $j \in K$ represents the relations between the input latent variables for root cause j , $\mathbf{b}_{f_{\text{att}}}^j$ is the corresponding bias, and \odot refers to the Hadamard product. Afterward, the output of this attention layer is used as the input for the following two fully connected layers to predict the root cause class label \mathbf{Y}^j :

$$f_{\text{clf}}^j(\mathbf{Z}) = a_{l_2}^j \left(\mathbf{W}_2^j \cdot \left(a_{l_1}^j \left(\mathbf{W}_1^j \cdot f_{\text{att}}^j(\mathbf{Z}) + \mathbf{b}_{l_1} \right) \right) + \mathbf{b}_{l_2}^j \right).$$

To predict multiple root causes simultaneously in an end-to-end manner, the training cross-entropy loss becomes $\mathcal{L}^{\text{Clf}} = -\sum_j Y_j \log(\text{softmax}(f_{\text{clf}}^j(\mathbf{Z})))$. The total loss for the MMSLA model is the summation of the VAE loss and classification loss: $\mathcal{L} = \mathcal{L}^{\text{VAE}} + \lambda \mathcal{L}^{\text{Clf}}$, where $\lambda \geq 0$ is the tuning parameter. The model is trained using the standard Adam optimizer, with hyperparameters fine-tuned via cross-validation to optimize generalization performance.

The proposed MMSLA model facilitates precise diagnosis of root causes across the three MII layers. To enable mitigation, we adapt established strategies from literature—tailored to data-, AI pipeline-,

and cyber-physical -layer hazards. A real-world case study (Sec. 3) details these mitigations and validates their efficacy through numerical experiments.

3 Case Study

To validate the resilient AI definition, diagnosis, and mitigation framework, we deployed an MII testbed in which the AI system supports the AJP quality modeling as its core computation task.

3.1 Experimental Setup

We utilize a collected real AJP dataset with a multivariate time series (MTS) classification DNN pipeline [Shojaee et al., 2021]. The dataset comprises 95 samples, each containing six *in situ* process variables (*i.e.*, atomizer gas flow, sheath gas flow, current, nozzle X-coordinate, nozzle Y-coordinate, and nozzle vibration) in time series format, alongside binary quality responses (*i.e.*, conforming or nonconforming) determined by the printed circuits’ resistance. We introduce four synthetic time series variables with negligible predictive power, resulting in ten total inputs for the classification task.

Using a simulation framework, we generate five datasets emulating distinct AJP machines. The AI pipeline (Sec. 1) includes data augmentation, standardization, and a DNN classifier, with 128 possible configurations. The optimal configuration, selected via training on the real dataset, serves as the baseline. By perturbing parameters in the baseline’s final layer, we derive five ground-truth models, each reflecting the underlying correlation between the input time series data and output quality response across simulated machines. These five models provide the ground truth label for the new input samples, which are generated by augmenting the original 95 samples with different methods (*i.e.*, timewrapping, pooling, convolving, *etc.*). Using the new samples and labels, the MTS DNN pipeline is trained for each machine. The top three performing pipelines among all configuration for each machine (3 pipelines times 5 machines equals 15 in total) are deployed on computation nodes to predict product-quality during the manufacturing process. The MII AI system’s computational infrastructure comprises five fog nodes (*e.g.*, Raspberry Pis) and a centralized Cloud server, resulting in six computation nodes in total.

To simulate the hazards in MII AI systems, we vary the levels of root cause factors from three layers to create different hazard scenarios. As shown in Table. 2, we introduce the following variations in the data layer: (i) Sensor contamination and failure are modeled by altering the ratio of affected sensors among ten input variables, replacing signals with constant values, or increasing/decreasing trends to mimic sensor degradation and calibration issues; (ii) Signal-to-Noise Ratio (SNR) is adjusted by injecting random noise into the input data at varying scales; (iii) Input distribution shifts are simulated by introducing a mixture of Gaussian-distributed data and controlling the resulting KL divergence from the original distribution; (iv) Class imbalance is manipulated by augmenting conforming samples and adjusting the nonconforming-to-conforming sample ratio (*i.e.*, 40/60, 25/75, 10/90) within each data batch. For the AI pipeline layer, we simulate pipeline singularity by forcing a subset of pipelines (0 of 3, 1 of 3, or 2 of 3) to produce identical predictions for all data points within a batch with doubled computation time. For the cyber-physical layer, we simulate communication channel disruption by initiating multiple simultaneous download and upload tasks on a subset of fog nodes (0 of 5, 1 of 5, or 2 of 5), mimicking a DDoS attack. Additionally, fog node failure is modeled by disabling a subset of fog nodes, preventing them from receiving or transmitting signals and halting their computation.

Table 2: The root cause factor levels.

Root Cause Factors	Definition	Layer	Level 0	Level 1	Level 2
Y_1	% of Contaminated or Failed Sensors	Data	0	10	20
Y_2	SNR	Data	Low	-	High
Y_3	Distribution Change of Input Variable	Data	Nan	Low	High
Y_4	Class Imbalancess	Data	40/60	25/75	10/90
Y_5	% of Sinular Pipelines	AI Pipeline	0	1	2
Y_6	% of Failed Egde Nodes	Cyber-physical	0	1	2
Y_7	% of Failed Communication Channels	Cyber-physical	0	1	2

In the experiment, each computation task is defined as predicting labels for a batch of data collected from a single machine. Each task is executed on one of six computation nodes. Using a full factorial design based on the factors in Table 2, we generate 1,458 normal and hazard scenarios. To reflect real manufacturing operations, where hazards are infrequent, we create five computation tasks per scenario, ensuring that at most two tasks per scenario experience hazard conditions (*i.e.*, at least one factor is not at Level 0). This results in a total of 7,290 computation tasks (1458×5). Each task is randomly assigned to a computation node by the Cloud.

After the execution of each computation task, \mathbf{X}^P are collected as the inference accuracy, precision, and F1 score of the top-3 pipelines on the data batch. Additionally, \mathbf{X}^R , runtime metrics, are captured at the same registration frequency throughout task execution, which include CPU utilization, CPU temperature, memory consumption, download bandwidth, upload bandwidth, and data transmission volume.

The hyperparameter λ is set as 0.1, and α is set as 0.1 by five-fold cross validation (CV). We have $u^R = u^P = 16$.

3.2 Evaluation of the Diagnosis Model

We first evaluate the MMSLA model’s diagnostic performance, focusing on detecting hazard conditions with one or multiple root causes. Assessing the failure severity level is left for future work.

Since the number of computation tasks under Level 2 and Level 3 for each root cause factor is much smaller than those under Level 0, there exists a class imbalance issue in the diagnosis task. Therefore, the F1 score is chosen as the evaluation metric. We compare the MMSLA model with three benchmark methods. The Multimodal Self Latent Attention (MSLA) model is a simplified version of MMSLA, using a single attention head instead of multiple heads. This head is applied to the latent feature \mathbf{Z} to predict multiple responses directly. Since no existing methods handle multimodal inputs with varying dimensions, we use Fourier transformation and summary statistics to extract features from \mathbf{X}^R , including sample length, harmonic mean, standard deviation, kurtosis, entropy, second harmonic, third harmonic, and total harmonic distortion. The extracted features, combined with \mathbf{X}^P , are used as inputs for Random Forest (RF) and XGBoost, two classical supervised learning models designed for high-dimensional complex data. To enhance the performance of RF and XGBoost, a separate model is trained for each root cause identification. As a result, five models are trained for

Table 3: The F1 score of root cause diagnosis for factor $Y_1 - Y_5$. Mean and standard deviation are reported over 5-fold CV.

Method	Y_1	Y_2	Y_3	Y_4	Y_5
MMSLA (Proposed)	0.90 (0.01)	0.70 (0.02)	0.89 (0.01)	0.94 (0.01)	0.95 (0.01)
MSLA	0.86 (0.02)	0.61 (0.01)	0.89 (0.01)	0.71 (0.01)	0.76 (0.02)
XGBoost + SMOTE	0.79 (0.00)	0.68 (0.01)	0.78 (0.01)	0.94 (0.01)	0.89 (0.00)
Random Forest+ SMOTE	0.62 (0.01)	0.56 (0.01)	0.70 (0.01)	0.95 (0.02)	0.95 (0.01)

Table 4: The F1 score of root cause diagnosis for factor Y_6, Y_7 . Mean and standard deviation are reported over 5-fold CV.

Method	Y_6	Y_7
XGBoost + SMOTE	0.90 (0.00)	0.89 (0.01)
Random Forest+ SMOTE	0.92 (0.01)	0.91 (0.01)

each of the two benchmark methods. To address the class imbalance, we apply SMOTE to augment the training data [Chawla et al., 2002]. However, SMOTE is not used for MMSLA and MSLA, as it degrades their performance, which might be due to that neural networks are more sensitive to the quality of augmented data.

We summarize the results for diagnosis factors Y_1 to Y_5 in Table 3. Y_6 and Y_7 are excluded because, under cyber-physical layer failure, the computation task cannot be completed, leading to missing \mathbf{X}^P . As a result, failures caused by these two factors are trivially identifiable and become a binary classification task. From the results in Table 3, the proposed MMSLA model achieves the best performance under four out of five factors. MSLA performs significantly worse than MMSLA and even underperforms the two benchmark methods for Y_4 and Y_5 . This may be due to the use of a single attention head, which blends heterogeneous variable dependencies across multiple root causes, limiting its ability to distinguish distinct factors. These results validate the effectiveness of the proposed multi-head self latent attention mechanism in capturing root cause-specific dependencies. In addition, both RF and XGBoost achieve high performance for Y_4 and Y_5 compared to other factors. This indicates that distribution change and class imbalance can be relatively easily diagnosed.

For the classification between factor Y_6 and Y_7 where \mathbf{X}^P is used as the input, both RF and XGBoost with SMOTE achieve satisfactory performance as shown in Table 4.

3.3 Resilience Metrics and Mitigation Strategies

Building on the diagnostic model’s outputs, we adapt context-aware mitigation strategies from literature tailored to the diagnosed hazard type (data-, AI pipeline-, or cyber-physical-layer), and quantify system recovery using the temporal and performance resilience metrics defined in Section 2.

For data-layer hazards, we implement automated data substitution, replacing corrupted inputs with data from a similar process [Whang et al., 2023]. This immediate mitigation stabilizes system performance, while root-cause-specific protocols, such as sensor recalibration for SNR degradation or synthetic oversampling for class imbalance, are initiated to address the diagnosed failure mode. In particular, the data generated for the same scenario for another machine but without hazards

is selected, where the machine is selected by the largest cosine similarity between the last layer parameters and the machine that generates the data with quality issues. Fig. 4 visualizes the AI system performance on a computation node under data layer hazards and the effect of the proposed mitigation strategy. A sequence of computation tasks is assigned to the node, with the X-axis representing the cumulative execution time and the Y-axis showing the F1 score of the product quality prediction task from the best result among the three deployed pipelines, reflecting the system’s performance. The diagnosis model is applied to monitor the system. The red point represents the task diagnosed with data-layer hazards, where the data are generated from Machine 1 (M1). After substituting the data source with M5, the performance recovers to the green point. Let $P_S = 0.75$ and $\Delta t = 400$ s as the average duration for each task is 360 s, the temporal and performance resilience can be calculated as: $FD = 664.58$, $PR = 0.598$, $RR = 0.822$. Since performance is recorded only upon task completion, the step function results in $t_1 = t_2$. As a result, recovery efficiency is not computed in this case.

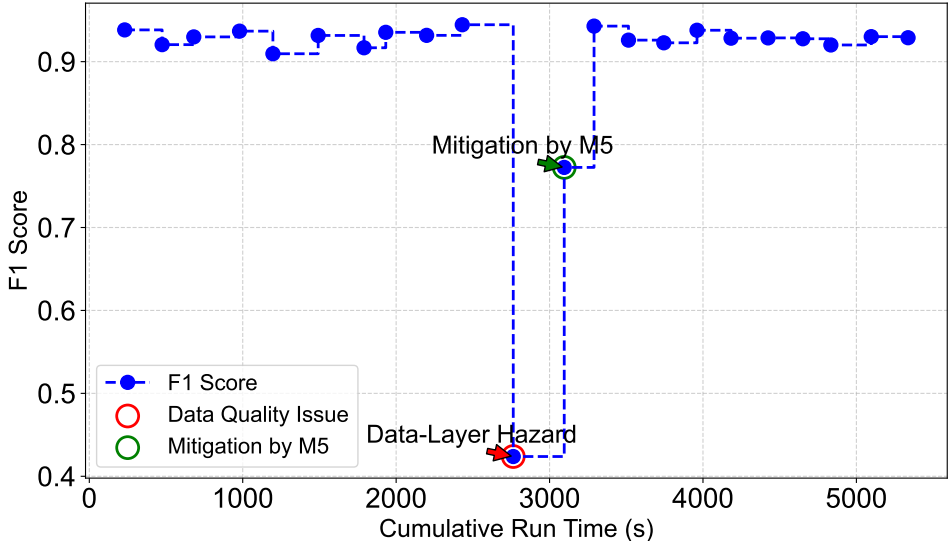


Figure 4: AI system performance under data hazards and mitigation.

For the hazards in the AI pipeline layer, we replace the pipeline with the ones from a similar machine (*i.e.*, the machine with the largest cosine similarity between the last layer parameters and the machine that faces pipeline singularity hazard). Similarly, Fig. 5 illustrates the MII testbed system performance on a computation node under pipeline layer hazards and the impact of replacing the pipelines with those from Machine 3 (M3). The corresponding temporal and performance resilience can be calculated as: $FD = 711.39$, $PR = 0.759$, $RR = 0.897$. Comparing PR and RR between the two mitigation actions in Fig. 4 and Fig. 5 reveals that the hazard in Fig. 4 is more severe, causing a greater impact on the AI system, as indicated by its lower PR and RR.

For cyber-physical layer hazards, when a fog node or communication channel failure is detected, the Cloud orchestrator dynamically reassigns the affected computation task to an available node, minimizing disruption and maintaining system resilience. The demonstration is omitted here due to the change in computation nodes.

The empirical results validate the effectiveness of mitigation strategies upon diagnosing the root causes from the literature and demonstrate the utility of the proposed resilience metrics in quantifying

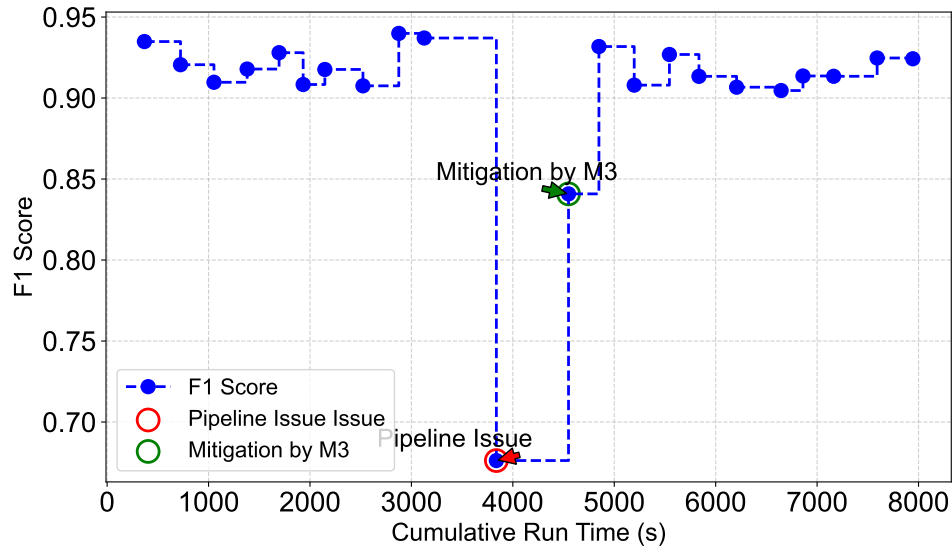


Figure 5: AI system performance under pipeline hazards and mitigation.

the AI system’s ability to withstand and recover from hazards in MII.

4 Conclusion and Future Work

With the growing adoption of AI systems in MII for critical decision-making, ensuring AI resilience has become a significant challenge for cybermanufacturing operations. However, there was a knowledge gap in defining AI resilience, identifying root causes of failures, and developing effective mitigation strategies. In this work, we propose a resilient AI framework for MII, focusing on the AI pipeline for online prediction tasks. We analyze AI performance under hazards from the data layer, AI pipeline layer, and cyber-physical layer, introducing temporal and performance resilience metrics to quantify system resilience. To enable accurate failure diagnosis, we develop the MMSLA model, which effectively captures dependencies within multimodal data of varying dimensions and accurately identifies specific root causes. Additionally, we propose layer-specific mitigation strategies to enhance system robustness. The effectiveness of the proposed resilient AI framework is validated through an MII testbed, where the MMSLA model outperforms multiple benchmark methods in diagnosis accuracy. As future work, we aim to develop a higher-resolution diagnosis model capable of detecting hazard severity levels and explore online mitigation strategies to further enhance AI system resilience in MII by improving data quality [Zeng et al., 2023a], AI pipeline uncertainty quantification and ranking [Chen and Jin, 2024], and computation offloading [Chen et al., 2018].

References

- Jorge F Arinez, Qing Chang, Robert X Gao, Chengying Xu, and Jianjing Zhang. Artificial intelligence in advanced manufacturing: Current status and future outlook. *Journal of Manufacturing Science and Engineering*, 142(11):110804, 2020.
- Christian Berger, Philipp Eichhammer, Hans P Reiser, Jörg Domaschka, Franz J Hauck, and Gerhard

- Habiger. A survey on resilience in the iot: Taxonomy, classification, and discussion of resilience mechanisms. *ACM Computing Surveys (CSUR)*, 54(7):1–39, 2021.
- Nitesh V Chawla, Kevin W Bowyer, Lawrence O Hall, and W Philip Kegelmeyer. Smote: synthetic minority over-sampling technique. *Journal of artificial intelligence research*, 16:321–357, 2002.
- Xiaoyu Chen and Ran Jin. Adapipe: A recommender system for adaptive computation pipelines in cyber-manufacturing computation services. *IEEE Transactions on Industrial Informatics*, 17(9): 6221–6229, 2020.
- Xiaoyu Chen and Ran Jin. Lori: Local low-rank response imputation for automatic configuration of contextualized artificial intelligence. *IEEE Transactions on Industrial Informatics*, 2024.
- Xiaoyu Chen, Lening Wang, Canran Wang, and Ran Jin. Predictive offloading in mobile-fog-cloud enabled cyber-manufacturing systems. In *2018 IEEE Industrial Cyber-Physical Systems (ICPS)*, pages 167–172. IEEE, 2018.
- Yao Cheng, Haitao Liao, and Elsayed A Elsayed. From reliability to resilience: More than just taking one step further. *IEEE Transactions on Reliability*, 2023.
- Peter Flach. Performance evaluation in machine learning: the good, the bad, the ugly, and the way forward. In *Proceedings of the AAAI conference on artificial intelligence*, volume 33, pages 9808–9814, 2019.
- Jim W Hall, Robert J Nicholls, Adrian J Hickford, and Martino Tran. Introducing national infrastructure assessment. 2016.
- Boris Hanin. Which neural net architectures give rise to exploding and vanishing gradients? *Advances in neural information processing systems*, 31, 2018.
- Diederik P Kingma. Auto-encoding variational bayes. *arXiv preprint arXiv:1312.6114*, 2013.
- Yifu Li, Xinwei Deng, Shan Ba, William R Myers, William A Brenneman, Steve J Lange, Ron Zink, and Ran Jin. Cluster-based data filtering for manufacturing big data systems. *Journal of Quality Technology*, 54(3):290–302, 2022.
- Jiahuan Liu, Fei Guo, Yun Zhang, Binkui Hou, and Huamin Zhou. Defect classification on limited labeled samples with multiscale feature fusion and semi-supervised learning. *Applied Intelligence*, pages 1–16, 2022.
- Yuehua Liu, Tharam Dillon, Wenjin Yu, Wenny Rahayu, and Fahed Mostafa. Missing value imputation for industrial iot sensor data with large gaps. *IEEE Internet of Things Journal*, 7(8): 6855–6867, 2020.
- Chi-Chun Lo, Chun-Chieh Huang, and Joy Ku. A cooperative intrusion detection system framework for cloud computing networks. In *2010 39th International Conference on Parallel Processing Workshops*, pages 280–284. IEEE, 2010.
- Douglas C Montgomery. *Statistical quality control*, volume 7. Wiley New York, 2009.
- Craig Poulin and Michael B Kane. Infrastructure resilience curves: Performance measures and summary metrics. *Reliability Engineering & System Safety*, 216:107926, 2021.
- Parshin Shojaee, Yingyan Zeng, Xiaoyu Chen, Ran Jin, Xinwei Deng, and Chuck Zhang. Deep neural network pipelines for multivariate time series classification in smart manufacturing. In *2021*

- 4th IEEE International Conference on Industrial Cyber-Physical Systems (ICPS)*, pages 98–103. IEEE, 2021.
- Hong Hui Tan and King Hann Lim. Vanishing gradient mitigation with deep learning neural network optimization. In *2019 7th international conference on smart computing & communications (ICSCC)*, pages 1–4. IEEE, 2019.
- Lening Wang, Yutong Zhang, and Ran Jin. A monitoring system for anomaly detection in fog manufacturing. In *2020 IEEE Conference on Industrial Cyberphysical Systems (ICPS)*, volume 1, pages 67–72. IEEE, 2020.
- Zhiguang Wang, Weizhong Yan, and Tim Oates. Time series classification from scratch with deep neural networks: A strong baseline. In *2017 International joint conference on neural networks (IJCNN)*, pages 1578–1585. IEEE, 2017.
- Steven Euijong Whang, Yuji Roh, Hwanjun Song, and Jae-Gil Lee. Data collection and quality challenges in deep learning: A data-centric ai perspective. *The VLDB Journal*, 32(4):791–813, 2023.
- Manzil Zaheer, Satwik Kottur, Siamak Ravanbakhsh, Barnabas Poczos, Russ R Salakhutdinov, and Alexander J Smola. Deep sets. *Advances in neural information processing systems*, 30, 2017.
- Yingyan Zeng, Xiaoyu Chen, and Ran Jin. Ensemble active learning by contextual bandits for ai incubation in manufacturing. *ACM Transactions on Intelligent Systems and Technology*, 15(1): 1–26, 2023a.
- Yingyan Zeng, Prithivrajan Thiyagarajan, Brian M Chan, and Ran Jin. Synthetic data generation and sampling for online training of dnns in manufacturing supervised learning problems. In *2023 IEEE 19th International Conference on Automation Science and Engineering (CASE)*, pages 1–6. IEEE, 2023b.